

High performance Lowpass Filter using Tetramerous Radial Stubs

S. Ali Sadeq, M. Hayati, H. Abbasi, S. Mohanad Mustafa, and F. Shama

Depart. of Electronic and Communication Eng., Faculty of Engineering, University of Kufa, Iraq

Depart. of Electrical Engineering, Razi University, Tagh-E-Bostan, Kermanshah-67149, Iran,

Depart. of Electrical Engineering, Ker.C., Islamic Azad University, Kermanshah, Iran

Depart. of Computer Technical Eng., College of Eng. and Tech., Al-Mustaqbal University, Babil, Iraq

Depart. of Electrical Engineering, Ker.C., Islamic Azad University, Kermanshah, Iran

salmaali19917@gmail.com, mohsen_hayati@yahoo.com, hamed.abbasi98@gmail.com,

sajjadmmj3@gmail.com, f.shama@aut.ac.ir

Corresponding Author : f.shama@aut.ac.ir

Abstract- This paper introduces a novel microstrip lowpass filter characterized by several remarkable features, including a sharp roll-off, extensive stopband, minimal insertion loss, compact dimensions, and high return loss, all achieved through the innovative use of tetramerous radial stub resonators. The transition band of the filter spans approximately 0.31 GHz, ranging from 1.96 to 2.27 GHz, with notable attenuation levels of -3 dB and -40 dB at the respective edges. Additionally, the stopband extends impressively from 2.2 GHz to 22 GHz, achieving attenuation greater than 20 dB, which ensures effective signal suppression outside the desired frequency range. In the passband, the insertion loss is exceptionally low, remaining below 0.1 dB, while the return loss exceeds 19.89 dB, indicating excellent matching characteristics. Furthermore, the total area of the filter measures a compact 189 mm², making it suitable for space-constrained applications. The proposed design has been fabricated and tested, with results from simulations and measurements demonstrating strong correlation and validating its performance.

Index Terms: low insertion loss, lowpass filter, tetramerous radial stubs resonator, ultra wide stopband.

I. INTRODUCTION

The microstrip-type lowpass filters have a crucial part in high-frequency communication systems, primarily because of its application in microwave filtering, the specifications of this type of filters such as performance, size, weight and cost are always a challenge to take over [1]. To have a compact low pass filter (LPF) with good characteristics, some different methods have been proposed. In reference [2], a microstrip lowpass filter utilizing a cascade of multiple resonators has been proposed.

This design features a sharp roll-off and a broad stopband, although it is relatively large in size. Reference [3] discusses a lowpass filter that employs stepped-impedance hairpin resonators, which achieves a sharp roll-off but suffers from poor return loss in the stopband and has a narrow stopband.

An innovative ultra-wide stopband lowpass filter utilizing transformed radial stubs (TRS) is explored in [4], which exhibits low return loss and high insertion loss. In [5], a microstrip lowpass filter that incorporates slit-loaded tapered resonators is introduced, noted for its very sharp rejection band, yet it is also large in size. Reference [6] presents a microstrip lowpass filter featuring triangular and high-low impedance resonators, characterized by sharp roll-off and a high figure of merit, but with unsatisfactory suppression levels in the stopband. Lastly, in [7], a microstrip lowpass filter combining triangular patch resonators and radial patch resonators is designed, offering an ultra-wide stopband and high return loss in the passband, though its roll-off and insertion loss are not ideal. In [8], an LPF with modified radial stub resonator has been presented which has extended stopband and remarkable roll-off, but their return and insertion losses in the passband are low and high, respectively. A microstrip lowpass filter with coupled rhombic stubs has been introduced in [9], which has wide stopband and compact size but it has not been matched in the passband and has a gradual roll-off. Reference [10] introduces a microstrip low-pass filter that utilizes multimode resonators. While it boasts a compact design and an ultra-wide stopband, its roll-off and rejection levels fall short of expectations. In [11], a wide rejection region LPF has been fabricated with remarkable characteristics except its large size. In [12], a wide LPF has been presented in planar form with significant return loss and very compact area but not such a very sharp band. In [13], a wide rejection band LPF has been fabricated using a complex and higher cost method of defected ground structure (DGS). Also, there is other high-cost and complex methods to design the LPFs such as ridge gap waveguide (RGW) [14] and coaxial transmission lines [15]. In addition, there are a lot of miniaturized planar simple-shaped LPFs as suppression cells for various types of harmonics eliminations with not appropriate performances in [16-26] for integrating with power dividers and power amplifiers. In [27], an unequal high performance microstrip LPF has been fabricated with non-reciprocal frequency responses.

This report presents a compact microstrip low-pass filter characterized by its straightforward design, sharp roll-off, ultra-wide stopband, minimal insertion loss, and high return loss within the passband. The filter features a tetramerous radial stub resonator along with tapered and rectangular suppression cells. It is fabricated on a substrate with a dielectric constant of $\epsilon_r = 2.2$, a thickness of 15 mil, and a loss tangent of 0.0009.

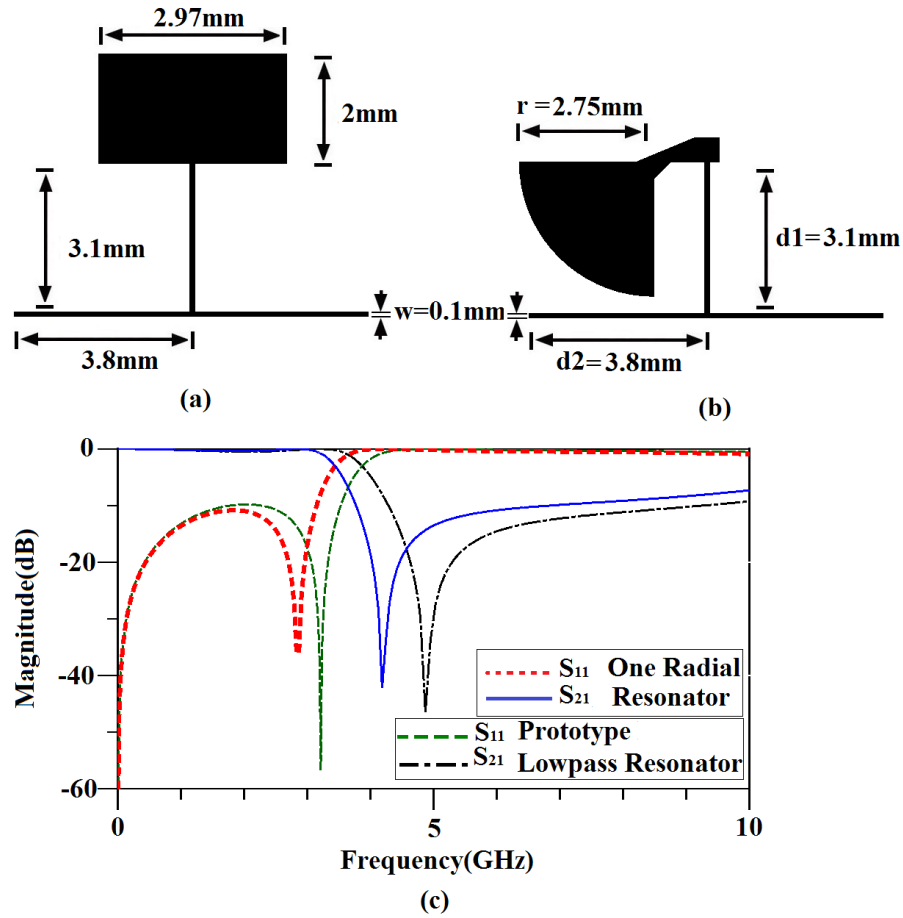


Fig. 1. (a) Prototype lowpass resonator structure (b) Radial resonator, (c) Compression of frequency response for one radial and prototype lowpass resonators.

II. FILTER DESIGN

The design methodology contains of two sections. At the first one, the proposed resonator which is tetramerous radial stubs resonator is designed, and at the second section to achieve wide stopband tapered and rectangular suppressing units are loaded to the main structure.

A. The tetramerous radial stubs resonator

At the began, a conventional stepped impedance resonator (CSIR) with Elliptic function response is designed [1]. The designed CSIR is shown in Fig. 1(a). To obtained an insertion loss with more attenuation at the resonant frequency and compact size at the same time, a modified radial stub resonator (MRSR) base on the designed CSIR is presented as shown in Fig. 1(b). The scattering parameter (S_{21}) of the MRSR and CSIR are shown in the Fig. 1(c). The cutoff frequency and resonance frequency is moved to the low range frequencies, by adding radial stubs to the MRSR, as

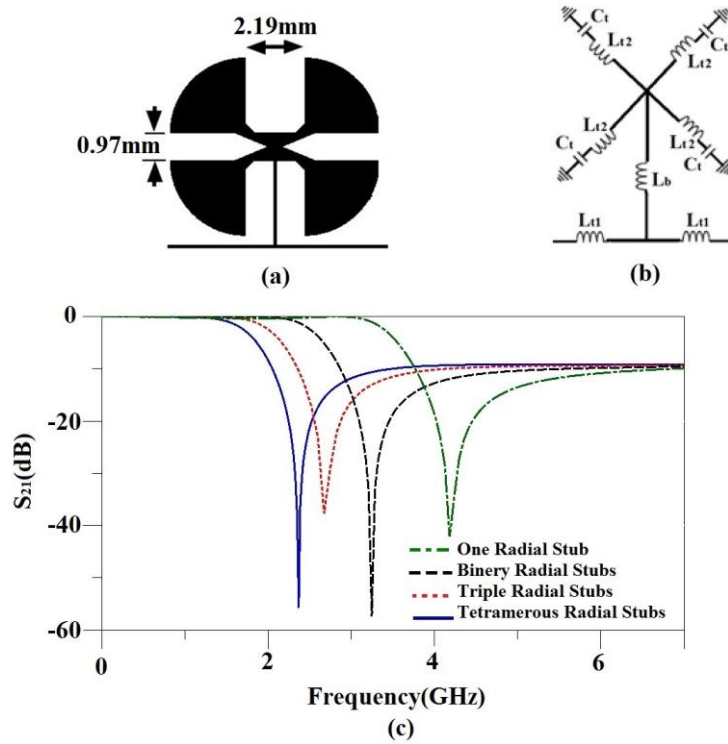


Fig. 2(a) Layout, (b) L-C equivalent, (c) Frequency response of tetramerous radial stubs resonator.

shown in Fig. 2(a). Also, the roll-off will be sharper when radial stubs add to the MRSR. The LC equivalent circuit for the MRSR with four radial stubs which is named tetramerous radial stubs resonator (TRSR) is shown in Fig. 2(b). The scattering parameter (S_{21}) for the MRSR with one, binary, triple and tetramerous radial stubs are shown in Fig. 2(c). Attenuation at the resonance frequency for the two radial stubs is better than one and four numbers is better than three, as illustrated in Fig. 2(c).

The scattering parameters for the TRSR is calculated using ABCD parameters which are:

$$S_{11} = S_{22} = \frac{\frac{m}{n} + \frac{(-m+n-j\frac{x_1 m}{n})}{z_0} - \frac{1}{z_0} - \frac{m}{n}}{\frac{m}{n} + \frac{(-m+n-j\frac{x_1 m}{n})}{z_0} + \frac{1}{z_0} + \frac{m}{n}} ; \quad S_{12} = S_{21} = \frac{2(\frac{m^2}{n^2} - (-m+n-j\frac{x_1 m}{n})\frac{1}{n})}{\frac{m}{n} + \frac{(-m+n-j\frac{x_1 m}{n})}{z_0} + \frac{1}{z_0} + \frac{m}{n}}, \quad (1)$$

where $m = jx_1 + jx_2 + \frac{Z}{4}$, $n = jx_2 + \frac{Z}{4}$, x_1 is the reactance of L_{t1} , x_2 is the reactance of L_b

and Z is the impedance of the each resonance branch of the TRSR LC equivalent circuit.

Equitation (1) shows, the effective elements in the S-parameters are L_b and C_t . d_1 and r are the related dimensions to the L_b and C_t .

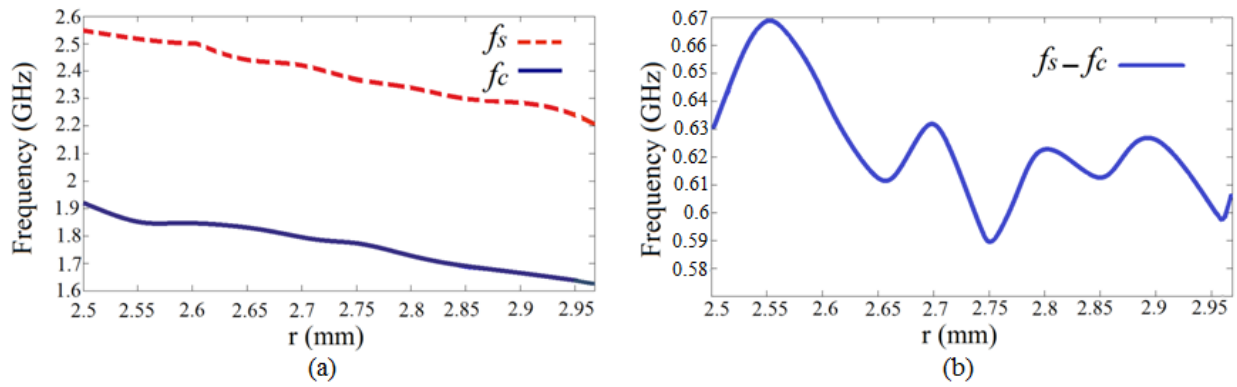


Fig. 3. (a) Variations of the f_s and f_c versus of the r . (b) Transition band versus r .

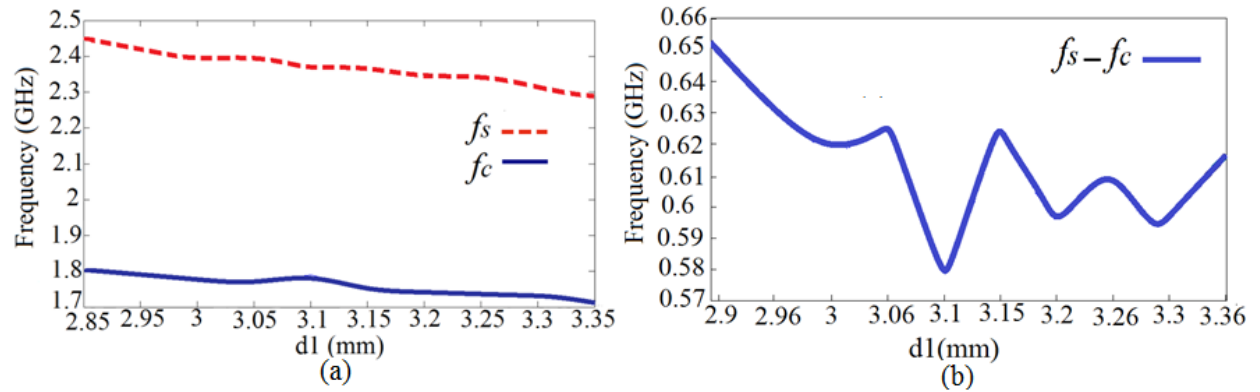


Fig. 4. (a) Variations of the f_s and f_c versus of the d_1 . (b) Transition band versus d_1 .

Fig. 3(a) shows the variations of the f_s and f_c versus of the r , where f_c and f_s are the cut off frequency and the resonance point of the resonator, respectively. The difference of the f_s and f_c which are transition band is shown in Fig. 3(b). It is clearly for the $r=2.75$ mm the transition band has the lowest value. Fig. 4(a) shows the variations of the f_s and f_c versus of the d_1 , the difference of the f_s and f_c which are transition band is shown in Fig. 4(b). It is clearly for the $d_1=3.1$ mm the transition band has the lowest value.

B. Suppressing cells design

In order to create a low-pass filter that features an extensive stopband, tapered stubs are employed as suppression cells, as illustrated in Fig. 5(a) and (b). The frequency response resulting from the integration of the proposed resonator with these tapered stubs is depicted in Fig. 5(c). The design of the T-shaped microstrip resonator, as well as the tapered structure used in the proposed low-pass filter, is grounded in the theoretical principles and mathematical relationships detailed in [1]. [1] provides comprehensive methodologies for modeling microstrip lines as equivalent inductive and capacitive elements, enabling accurate determination of physical dimensions based on the desired frequency response. In this work, the tapered structure is employed instead of the conventional

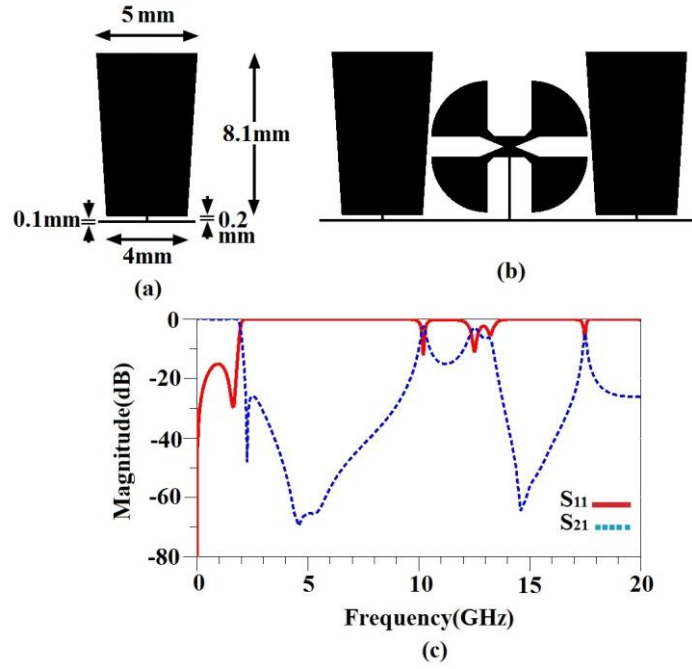


Fig. 5(a) Layout of tapered suppressing cells. (b) The proposed resonator and the tapered suppressing cell together (c) its frequency response.

horizontal arm in the T-shaped resonator to enhance the capacitive effect, while maintaining an identical total. Using standard techniques involving characteristic impedance and electrical length, the physical dimensions of each resonator section are precisely calculated to achieve the desired cutoff behavior. The entire design process relies on normalized element values extracted from standard low-pass prototype tables, as provided in [1]. These values are used to determine the impedance ratios and scaling factors for each segment, ensuring the filter structure meets the required specifications. By following this systematic design approach, the resonator achieves accurate frequency response and high fabrication reliability.

To enhance the stopband and eliminate harmonics in the 9 to 14 GHz range, two rectangular stubs have been incorporated into the design, as expressed in Fig. 6(a) and (b). The completed layout and S-parameters graph of the proposed filter are presented in Fig. 6(b) and (c), respectively. The rectangular stubs used in the proposed structure are also designed following the same theoretical framework described in [1], similar to the T-shaped resonator. This reference outlines the modeling of rectangular stubs as capacitive elements in microstrip structures and provides analytical methods for calculating their physical dimensions. Given a desired capacitance value at a specific point in the filter, the width of the rectangular stub can be selected, and the corresponding length determined accordingly. This design procedure is based on the relationships between characteristic impedance,

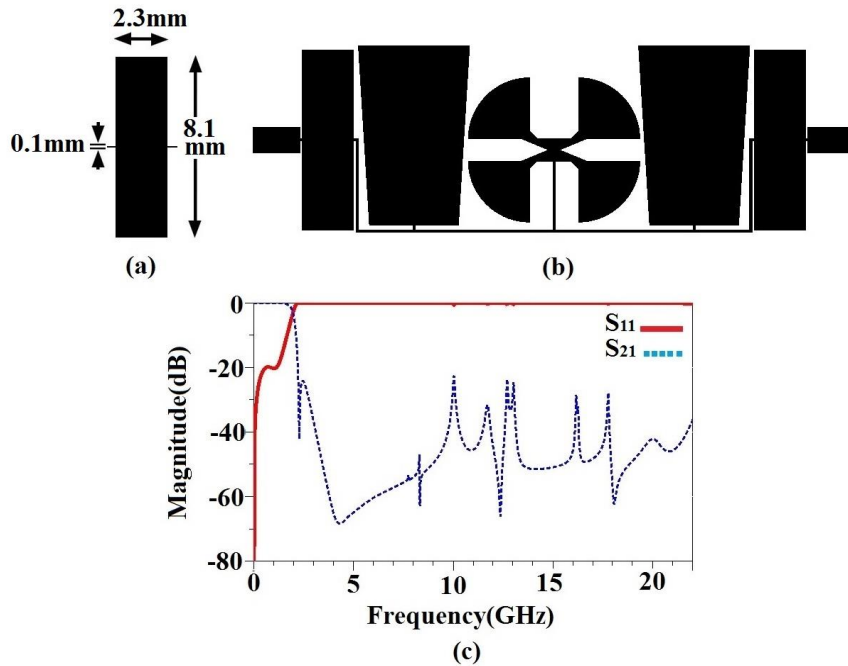


Fig. 6. (a) Rectangular cells. (b) Proposed filter. (c) Simulated results

physical length, and the target operating frequency, all of which are clearly defined in Reference [1]. In this work, two rectangular stubs are incorporated into the filter to enhance harmonic suppression and improve stopband performance in the 9–14 GHz range. These stubs are carefully sized to generate the required capacitive effect within this frequency band. By choosing appropriate widths and applying the design methods outlined in [1], the physical lengths of the stubs are computed to meet performance targets. Overall, the design of these elements strictly adheres to established microwave filter synthesis techniques and ensures effective stopband extension and harmonic rejection.

III. FINAL RESULTS

Fig. 7(a) and (b) display the layout and photograph of the fabricated filter, respectively. The simulated and measured performance of the filter is illustrated in Fig. 7(c). It is evident that the stopband attenuation extends from 2.2 GHz to 22 GHz, exceeding -20 dB. The filter demonstrates a low insertion loss (IL) of under 0.1 dB, while the return loss (RL) exceeds 19.89 dB within the passband. The transition band spans 0.31 GHz, ranging from 1.96 to 2.27 GHz, with corresponding attenuation levels of -3 dB and -40 dB, respectively. An overall performance review is summarized in Table I, with parameters defined in [12].

Table I. An overall performance review

Ref.	f_c	ζ	RSB	NCS	SF	FOM	IL	RL	$OFOM$
[2]	2.4	92.5	1.355	0.037	3	10106	0.3	11	370.553
[3]	2.02	63.8	1.2	0.05	3.3	5052	0.3	15	252.600
[5]	1.78	168	1.4	0.04	1	5880	0.3	10.67	209.132
[7]	1	37	1.65	0.01	1.5	9065	0.4	18	407.92
[8]	1.19	72.15	1.71	0.0123	2	23873.5	0.26	14	1285.5
[9]	1.75	57.8	1.61	0.012	3	27142	0.5	11	597.124
This work	1.96	119.354	1.64	0.014	2.3	32157.6	0.1	19.89	6396.14

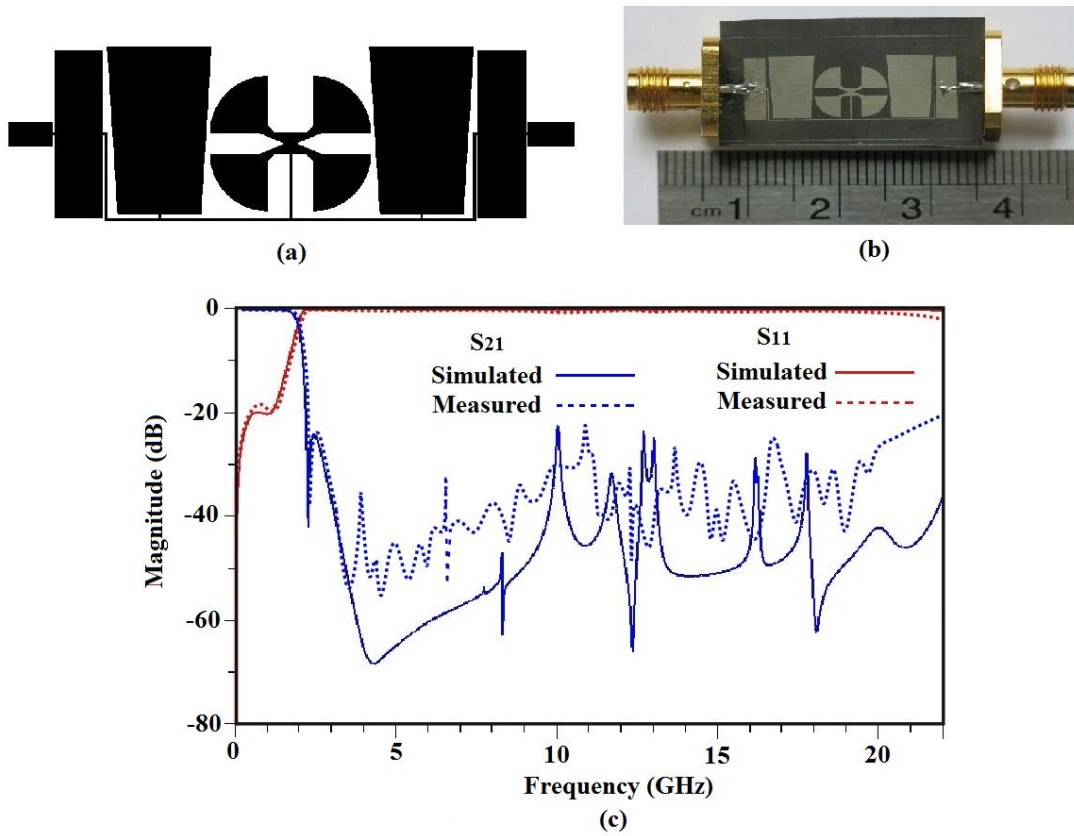


Fig. 7. (a) LPF structure (b) Fabricated circuit (c) Results graphs

Consequently, the comparison indicates that the proposed filter outperforms those referenced in the literature in terms of figure of merit (FOM), overall figure of merit (OFOM), return loss (RL), and insertion loss (IL).

IV. CONCLUSION

A lowpass filter featuring a cut-off frequency of 1.96 GHz was designed, manufactured, and tested using a tetrameric radial stub resonator. This lowpass filter exhibits several advantageous characteristics, including an exceptionally wide stopband, a steep roll-off, and a compact form factor. The rectangular and tapered cells were used as suppressing cells in this LPF. The OFOM for the proposed filter was calculated, it is equal to 6396.14 which is shown good overall performance. The results show, the designed LPF is a remarkable choice for using in communication systems.

REFERENCES

- [1] M. Lancaster and J.-S. Hong, *Microstrip filters for RF/microwave applications*, 1st ed. 2001. ISBN: 0-417-38877-7.
- [2] J.-L. Li, S.-W. Qu, and Q. Xue, "Compact microstrip lowpass filter with sharp roll-off and wide stopband," *Electron. Lett.*, vol. 45, no. 2, pp. 110–111, Jan. 2009.
- [3] L.-H. Hsieh and K. Chang, "Compact elliptic-function low-pass filters using microstrip stepped-impedance hairpin resonators," *IEEE Trans. Microw. Theory Techn.*, vol. 51, no. 1, pp. 193–199, Jan. 2003.
- [4] K. Ma and K. S. Yeo, "New ultra wide stopband low-pass filter using transformed radial stubs," *IEEE Trans. Microw. Theory Techn.*, vol. 59, no. 3, pp. 604–611, Mar. 2011.
- [5] M. Hayati and A. Lotfi, "Elliptic-function lowpass filter with sharp cutoff frequency using slit-loaded tapered compact microstrip resonator cell," *Electron. Lett.*, vol. 46, no. 2, Jan. 2010.
- [6] J. Wang et al., "Miniaturised microstrip lowpass filter with broad stopband and sharp roll-off," *Electron. Lett.*, vol. 46, no. 8, pp. 573–575, Apr. 2010.
- [7] J. Wang, H. Cui, and G. Zhang, "Design of compact microstrip lowpass filter with ultra-wide stopband," *Electron. Lett.*, vol. 48, no. 14, pp. 854–856, July 2012.
- [8] M. Hayati, M. Khodadoost, and H. Abbasi, "Microstrip lowpass filter with wide stopband and sharp roll-off using modified radial stub resonator," *Int. J. Microw. Wireless Technol.*, in press, 2016.
- [9] B. Zhang et al., "Compact lowpass filter with wide stopband using coupled rhombic stubs," *Electron. Lett.*, vol. 51, no. 3, pp. 264–266, Feb. 2015.
- [10] Q. Li et al., "Compact ultra-wide stopband low pass filter using multimode resonators," *Electron. Lett.*, vol. 51, no. 14, pp. 1084–1085, July 2015.
- [11] S. Soltani, H. Pakniat, and N. Yasrebi, "A wide stopband, high selectivity microstrip low-pass filter for wireless communications," *AEU Int. J. Electron. Commun.*, vol. 155443, Jan. 2024.
- [12] S. M. Mustafa et al., "Compact microstrip lowpass filter with wide stopband and sharp transition band using radial stub resonator," *AEU Int. J. Electron. Commun.*, vol. 155468, Jan. 2024.
- [13] E. G. Ouf, A. S. Abd El-Hameed, and E. A. Abdallah, "Compact lowpass filter with vast out-of-band rejection utilizing DGS," *AEU Int. J. Electron. Commun.*, vol. 177, p. 155207, Jan. 2024.
- [14] M. Gadelrab, S. I. Shams, M. Elsaadany, and A. Sebak, "Ridge Gap Waveguide Low Pass Filters: A Systematic Design Approach," *IEEE Access*, doi: 10.1109/ACCESS.2024.3411393, Jan. 2024.
- [15] E. Yılmaz and M. Üçüncü, "Coaxial low-pass filter design and manufacture," *IEEE Access*, vol. 11, pp. 15845–15854, Feb. 2023.

-
- [16] B. Hiedari and F. Shama, "A harmonics suppressed microstrip cell for integrated applications," *AEU Int. J. Electron. Commun.*, vol. 83, pp. 519–522, Jan. 2018.
- [17] R. Pouryavar, F. Shama, and M. A. Imani, "A miniaturized microstrip Wilkinson power divider with harmonics suppression using radial/rectangular-shaped resonators," *Electromagnetics*, vol. 38, no. 2, pp. 113–122, Feb. 2018.
- [18] E. Jedkare, F. Shama, and M. A. Sattari, "Compact Wilkinson power divider with multi-harmonics suppression," *AEU Int. J. Electron. Commun.*, vol. 127, p. 153436, Apr. 2020.
- [19] M. A. Imani, F. Shama, M. Alirezapoori, and M. Ekhteraei, "Miniaturized microstrip lowpass filter using cylindrical-shaped resonators for integrated applications," *Analog Integr. Circuits Signal Process.*, vol. 95, pp. 223–229, Jan. 2018.
- [20] M. Hayati and F. Shama, "A high-efficiency narrow-band class-F power amplifier integrated with a microstrip suppressing cell," *Analog Integr. Circuits Signal Process.*, vol. 90, pp. 351–359, Oct. 2017.
- [21] M. Hayati, F. Shama, and M. Ekhteraei, "Miniaturized microstrip suppressing cell with wide stopband," *Appl. Comput. Electromagn. Soc. J. (ACES)*, pp. 1244–1249, 2016. (Month unspecified.)
- [22] M. A. Imani, F. Shama, and G. H. Roshani, "Miniaturized Wilkinson power divider with suppressed harmonics," *Microw. Opt. Technol. Lett.*, vol. 62, no. 4, pp. 1526–1532, Apr. 2020.
- [23] M. A. Imani, F. Shama, M. Alirezapoori, S. Haghiri, and A. Ghadrddan, "Ultra-miniaturized Wilkinson power divider with harmonics suppression for wireless applications," *J. Electromagn. Waves Appl.*, vol. 33, no. 14, pp. 1920–1932, Jul. 2019.
- [24] A. Hosseini Tabatabaee, F. Shama, M. A. Sattari, and S. Veysifard, "A miniaturized Wilkinson power divider with 12th harmonics suppression," *J. Electromagn. Waves Appl.*, vol. 35, no. 3, pp. 371–388, Feb. 2021.
- [25] S. Veysifard and F. Shama, "Miniaturized Gysel power divider with nth harmonics suppression," *AEU Int. J. Electron. Commun.*, vol. 95, pp. 279–286, Jan. 2018.
- [26] M. Hayati and F. Shama, "High efficiency class-F power amplifier integrated with microstrip asymmetric lowpass filter," *Analog Integr. Circuits Signal Process.*, vol. 98, pp. 587–596, Apr. 2019.
- [27] F. Shama, M. Hayati, and M. Ekhteraei, "Compact microstrip lowpass filter using meandered unequal T-shaped resonator with ultra-wide rejection band," *AEU Int. J. Electron. Commun.*, vol. 85, pp. 78–83, Feb. 2018.